Coupled geomechanics and flow simulation for time-lapse seismic modeling

Susan E. Minkoff, Charles M. Stone, J. Guadalupe Arguello, Sandia National Labs, Steve Bryant, Joe Eaton, Malgo Peszynska, Mary Wheeler, University of Texas at Austin*

Summary

Time-lapse seismic feasibility studies for compactible reservoirs such as Ekofisk in the North Sea require coupled flow simulation and geomechanical deformation modeling. In this paper we present an algorithm for 2-way coupling of flow and geomechanics and indicate what impact the coupled code has on calculation of seismic velocities and density. Each of the simulators — the reservoir simulator from the University of Texas and the geomechanics code from Sandia National Labs — was developed under the US DOE's ACTI program. The codes use 3D finite element discretizations and can be run in parallel. The flow simulator can account for faults and multiple flow models in a single simulation. The geomechanics code models contacts and large, inelastic deformations. We modify the black oil system to include changes in the reservoir geology (porosity) during a single simulation while still maintaining conservation of mass. Modifications to the geomechanics code allow changes in pore pressure to be included in the total stress calculation. The geomechanics code produces volumetric strain-induced porosity updates for the flow simulator. By allowing the two simulators to have different spatial grids and to take different time steps, we are able to account for physical differences in resolution between flow and geomechanics. A plastic cap constitutive model provides a realistic mechanism for capturing subsidence due to production-induced pressure drops. We demonstrate the coupled code with a synthetic example based on a diatomite reservoir in the Belridge Field, California. Ten years of primary production results in almost a foot of subsidence at the wells. Correspondingly, we see a 2-4% change in reservoir porosity during the simulation. Calculation of saturated rock seismic velocities and density using the coupled simulation are more realistic than calculation of elastic rock properties from flow only.

Introduction

Simulation of oil field production in highly compactible weak-formation reservoirs such as Ekofisk in the North Sea and Belridge in California must be able to capture large, inelastic deformations arising from changes in reservoir pressure. Flow simulators typically handle changes in reservoir geology through rock compressibility — inadequate for areas with substantial subsidence and compaction.

Coupled geomechanics and reservoir simulation provides a more sophisticated model of reservoir deformation during production and typically falls into one of three categories — full coupling, loose coupling, and one-way coupling. Fully coupled simulators, theoretically the most accurate, solve a single set of equations over a single grid. (See Lewis and Sukirman (1993) for an example.) In loose coupling, output from each simulator is periodically used as input by the other (2-way coupling). The advantages of loose coupling include the flexibility to make use of more sophisticated simulators, and the ability to allow for resolution differences in gridding and time stepping (see Settari and Mourits (1994)). In one-way coupling (the easiest to implement but the least realistic physically), the flow simulator output (pore pressures) are used in the geomechanics calculation, but no corresponding reservoir geology change is incorporated into the flow simulation (see Minkoff et al. (1999)).

In this work, we describe a loose, staggered in-time, 2-way coupling scheme currently implemented as follows:

Repeat for $i = 1, \ldots, n-1$ *where* $T_n = T_{final}$*:*

1. $\Delta t = t_{i+1} - t_i$
2. *Given the current reservoir geology (permeability* K_c*, porosity* ϕ_c*), run flow simulation for time* Δt*. Output updated pore pressure* P_+*.*
3. *Calculate the total mechanical stress incorporating the new pore pressure* P_+*, and run geomechanics for time* Δt*. Output porosity update* ϕ_+*.*
4. *Replace* ϕ_c *by* ϕ_+*.*

In the remainder of this paper, we describe the black oil model reservoir simulator, the geomechanical deformation code, and modifications to the two simulators for 2-way coupling. In the context of time-lapse seismic modeling, we describe a synthetic example based on part of the Belridge Field. The intent is to illustrate the impact of coupled geomechanics and reservoir flow simulation on time-lapse data.

Reservoir Simulation

The fluid flow simulator, *IPARS*, built at the University of Texas, includes multiple physical models—2-phase hydrology, 3-phase black oil, and compositional (see Wheeler et al. (1999)). We use the isothermal, black oil model to simulate the flow of oil, gas, and water. The black oil model code is fully implicit, 3-D, parallel, and uses an extended mixed finite element method to maintain local conservation of mass.

Given that N_i is the stock tank volume of component i ($i = o, g, w$) per unit pore volume, ϕ is porosity, R_o is the

stock tank volume of gas dissolved in a stock tank volume of oil, and q_i = the total stock tank rate of injection of phase i, the mass balance equations are

$$\frac{\partial}{\partial t}(\phi N_g) = \nabla \cdot (U_g + R_o U_o) + q_g$$

$$\frac{\partial}{\partial t}(\phi N_i) = \nabla \cdot U_i + q_i \qquad i = oil, water$$

Darcy's Law gives the mass velocity U of phase i:

$$U_i = \frac{K k_{ri}}{B_i \mu_i} \cdot (\nabla P_i - \rho_i g \nabla D).$$

Here, K is the diagonal permeability tensor, and k_{ri} is the relative permeability of phase i. B_i is the formation volume factor for phase i. P_i is pressure, μ_i is viscosity, and ρ_i is density. Gravity has magnitude g, and D is depth.

Porosity changes are typically captured via the linear expression

$$\phi = \phi_z(1 + c_r P_w)$$

with ϕ_z the porosity as a function of space only, and the rock compressibility, c_r, a constant. In reality, conventional black oil simulators assume the reservoir geology (porosity and permeability) are changing very little (if at all) during flow simulation.

The nonlinear system resulting from the finite element discretization requires an iterative solution of the Newton system $Jx = -R$, with J the Jacobian matrix of partial derivatives with respect to the primary variables $x = [P_w, N_o, N_g]$, and R the residual.

For coupled geomechanics/reservoir simulation, we incorporate porosity updates at time step n through the residual modification

$$R = (\phi x)^n - (\phi x)^{n-1} - dt(\nabla \cdot U^n + q^n).$$

In the above formulation, mass is conserved, and the Newton update accounts for a decrease in porosity (for example) by increasing the well rates and pressures at the next time step.

Geomechanical Deformation Modeling

The geomechanics code from Sandia National Labs, *JAS3D*, is 3-D, parallel, and uses a finite element discretization (Arguello et al., 1998). The simulator maintains equilibrium by matching the divergence of the stresses σ_{ij} against the body forces b_i with the density ρ:

$$\partial \sigma_{ij}/\partial x_j + \rho b_i = 0.$$

Here x_j is the position vector, and we impose kinematic and traction boundary conditions on the boundary of the body.

In this study we use the modified Sandler-Rubin cap/plasticity constitutive model illustrated in Figure 1 (see Fossum et al. (1995)). This model has an isotropic loading function which contains two major components: the failure envelope and the elliptical cap. The failure envelope portion of the loading function has the following form:

$$h(I_1, \sqrt{J_2}, \Psi) = \Gamma\sqrt{J_2} - [A - C\exp(BI_1)] = 0$$

Where A, B, C are material constants; $I_1 = \sigma_{kk}$ and $\sqrt{J_2} = \sqrt{(s_{ij}s_{ij}/2}$ with s_{ij} the stress deviator. The Lode-angle dependence of yield is given by:

$$\Gamma = \{[1 + \sin(3\Psi)] + [1 - \sin(3\Psi)]/K^*\}/2$$

Where K^* is the ratio of the yield stress in triaxial extension to triaxial compression. The Lode angle is

$$\Psi = \frac{1}{3}\arcsin\left(-\frac{27}{2}\frac{J_3}{(3J_2)^{3/2}}\right)$$

for $-\pi/6 \le \Psi \le \pi/6$. J_3 is the third invariant of the deviator stress. For triaxial extension, $\Psi = -\pi/6$ and for triaxial compression, $\Psi = \pi/6$. The Strain-Hardening (cap surface) is of the form:

$$H(I_1, \sqrt{J_2}, \Psi, \kappa) =$$

$$\Gamma\sqrt{J_2} - \frac{1}{R}\sqrt{[X(\kappa) - L(\kappa)]^2 - [I_1 - L(\kappa)]^2}$$

Where R denotes the ratio of the major to minor axis in the elliptical cap. The cap is chosen so that the tangent at its intersection with the failure envelope is horizontal. $-X(\kappa)$ and $-L(\kappa)$ define the intersections of the elliptic cap with the I_1 axis and the failure envelope, respectively.

$$\kappa = \epsilon^p_{kk} =$$

$$W\left\{\exp[D_1(X(\kappa) - X_0) - D_2(X(\kappa) - X_0)^2] - 1\right\}$$

With W defining maximal plastic volumetric compaction the material can experience under hydrostatic loading. X_0 the initial cap position; and D_1, D_2 material parameters.

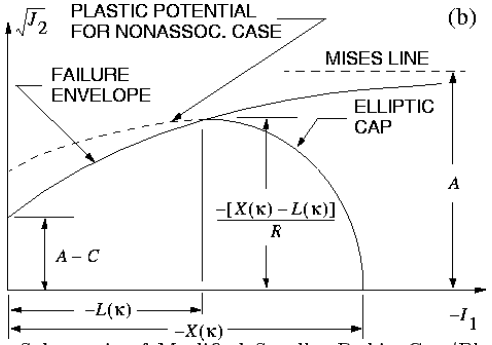

Fig. 1: Schematic of Modified Sandler-Rubin Cap/Plasticity constitutive model.

Coupled geomechanics and flow simulation

The reservoir simulator provides pore pressures which are included in the total stress calculation

$$\sigma_{ij}^T = \sigma_{ij} + p\delta_{ij}.$$

With p the pore fluid pressure, δ_{ij} is the Kronecker delta function, and σ_{ij} is the "effective" stress that the rock is subjected to. On output, the geomechanics code provides porosity updates via the following relative density calculation:

$$\phi = 1 - \frac{\rho}{\rho_0}(1 - \phi_0)$$

Here ρ is the current density, ρ_0 is the initial density, ϕ_0 the initial porosity, ϵ_v the volume strain, and

$$\frac{\rho}{\rho_0} = \log(\epsilon_v).$$

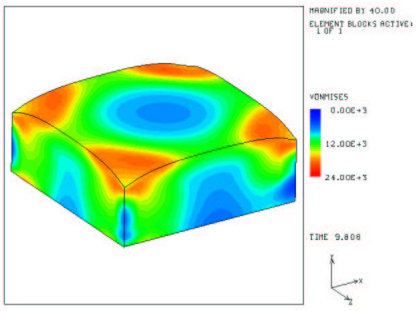

Fig. 2: Von Mises stress determined at 10 years of coupled flow/geomechanics (in lb/ft^2).

Time-Lapse Seismic Modeling

We use Gassmann's equations to convert the time-dependent reservoir pressures and saturations resulting from the flow simulation (or flow simulation and geomechanics) into elastic rock parameter changes (Lumley (1995)). Gassmann's equations provide a way to compute the effective bulk and shear moduli (K and μ respectively) of reservoir rock saturated with a given composition of pore fluids from the elastic moduli of the dry rock. These equations are

$$\mu_{sat} = \mu_{dry}$$

$$\frac{K_{sat}}{K_{solid} - K_{sat}} = \frac{K_{dry}}{K_{solid} - K_{dry}} + \frac{K_{fluid}}{\phi(K_{solid} - K_{fluid})}$$

They require knowledge of the effective bulk modulus of the pore fluid K_{fluid} (a function of both pressure and saturation), the porosity ϕ (possibly a function of deformation), the bulk and shear moduli of the dry rock with empty pores K_{dry}, μ_{dry} (functions of pressure), and the bulk modulus of the mineral material making up the rock K_{solid}.

We calculate the fluid phase bulk modulus and density by

$$\begin{aligned} \frac{1}{K_{fluid}} &= \frac{S_w}{K_w} + \frac{S_o}{K_o} + \frac{S_g}{K_g} \\ \rho_{fluid} &= S_w\rho_w + S_o\rho_o + S_g\rho_g. \end{aligned}$$

From Gassmann's equations and relationships between elastic parameters we can determine the density ρ, compressional wave velocity V_p, and shear wave velocity V_s at a given fluid saturation, pressure, and porosity.

A Numerical Example

Belridge Field, 50 miles west of Bakersfield, California, was the fifth most productive field in the US (1996 status). The field contains a 1000 ft. thick diatomite reservoir with very high porosity (45-70%) and very low permeabilities ($\sim$ .1 mD). Production-induced pressure drops resulted in 10–15 ft. of compaction in the extremely weak diatomite as well as numerous well failures (Fredrich et al., 1996).

Diatomite is approximately 15x weaker than sandstone, and our synthetic example is based on the weakest of the eight diatomite layers in the Belridge Field.

The reservoir has 4 production wells in the corners of the 346x346x144 ft. domain completed to different depths. Initial water saturation was taken to be 35% and initial pore pressure at 1185 ft. (top of the reservoir layer) was 545 psi. The initial porosity and permeability were 50% and .1 mD respectively, and we used 29 API gravity reservoir oil. The simulation ran for 10 years with flow time steps of .2–2 days and geomechanics time steps of 20 days.

At the end of the 10-year run, pressures at the top of the reservoir had dropped to 250 psi causing gas to come out of solution and vertical subsidence of 10 inches. Decreased pore pressure resulted in final porosities as low as 48% at the wells. The heavy oil and low permeability caused very slow flow and little interaction between wells. The von Mises stress computed by the geomechanics code at 10 years flow is plotted on a deformed mesh as shown in Figure 2.

Using Gassmann's equations, we made time-lapse seismic estimates of changes in saturated rock elastic properties during the simulation. The high volume of pore fluid (50%) and low moduli of diatomite (on the order of the pore fluids) caused substantial time-lapse changes evident in the seismic velocities. The decrease in fluid density and pore pressure (increase in differential pressure) caused a 12% increase in V_p at the top of the wells and a corresponding decrease at the bottom (below the well completion level). Saturated rock density difference between 10 years and one month of coupled flow/geomechanics is shown in Figure 3. (Figures 3–5 show the reservoir rotated 90 degrees). Figures 4 and 5 give the difference in saturated rock density and velocity calculated with geomechanics/flow vs. just flow at 10 years. The coupled simulation produces changes in porosity which in turn

affect the resulting flow simulation saturations and pressures. Although the velocity difference owing to deformation is minor in this example, the density difference is on the same order as the time-lapse change. Flow without geomechanics over-estimates the decrease in saturated rock density.

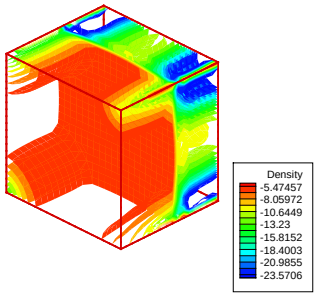

Fig. 3: Difference between saturated rock density at 10 years and 1 month of coupled flow simulation/geomechanics (in kg/m^3).

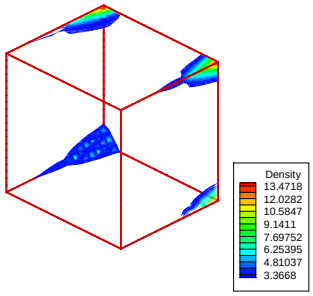

Fig. 4: Difference between saturated rock density at 10 years calculated with and without geomechanics (in kg/m^3).

Acknowledgements

We thank Joanne Fredrich (SNL) for providing rock physics data on Belridge diatomite. The Sandia researchers are supported by the U.S. DOE under Contract DE-AC04-94AL85000. Susan Minkoff receives funding for this work through DOE's MICS Office. Sandia is a multiprogram laboratory operated by Sandia Corporation, a Lockheed Martin Company. Researchers at UT are grateful to Qin Lu for work on the black oil model and thank the DOE (grant # 951522401), NGOTP, and sponsors of the Industrial Affiliates Program at the Center for Subsurface Modeling.

References

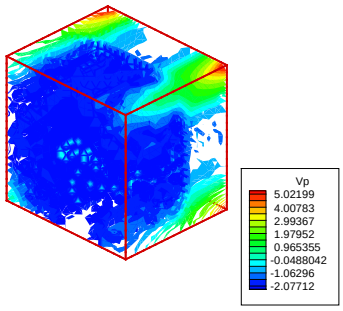

Fig. 5: Difference between saturated rock compressional wave velocity at 10 years calculated with and without geomechanics (in m/s).

Arguello, J., Stone, C., and Fossum, A., 1998, Progress on the development of a three-dimensional capability for simulating large-scale complex geologic processes: 3rd North American Rock Mechanics Symposium, ISRM, Exp. Abst.

Fossum, A., Senseny, P., Pfeifle, T., and Mellegard, K., 1995, Experimental determination of probability distributions for parameters of a salem limestone cap plasticity model: Mechanics of Materials, **21**, 119–137.

Fredrich, J., Arguello, J., Thorne, B., Wawersik, W., Deitrick, G., de Rouffignac, E., Myer, L., and Bruno, M., 1996, Three-dimensional geomechanical simulation of reservoir compaction and implications for well failures in the Belridge Diatomite: Ann. Tech. Conf., SPE, Exp. Abst., 195–210.

Lewis, R., and Sukirman, Y., 1993, Finite element modelling of three-phase flow in deforming saturated oil reservoirs: Int. J. Num. and Anal. Meth. in Geomech., **17**, 577–598.

Lumley, D., 1995, Seismic time-lapse monitoring of subsurface fluid flow: Ph.D. thesis, Department of Geophysics, Stanford University, Stanford, CA.

Minkoff, S., Stone, C., Arguello, J., Bryant, S., Eaton, J., Peszynska, M., and Wheeler, M., 1999, Staggered in time coupling of reservoir flow simulation and geomechanical deformation: Step 1 — one-way coupling: Res. Sim. Symp., SPE, Exp. Abst., 329–330.

Settari, A., and Mourits, F., 1994, Coupling of geomechanics and reservoir simulation models *in* Siriwardane, and Zaman, Eds., Computer Methods and Advances in Geomechanics:: Balkema, 2151–2158.

Wheeler, M., Arbogast, T., Bryant, S., Eaton, J., Lu, Q., Peszynska, M., and Yotov, I., 1999, A parallel multiblock/multidomain approach for reservoir simulation: Res. Sim. Symp., SPE, Exp. Abst., 51–61.